Article

Modeling Spin Interactions in a Cyclic Trimer and a Cuboidal CoO Core with Co(II) in Tetrahedral and Octahedral Environments

John F. Berry, F. Albert Cotton, Chun Y. Liu, Tongbu Lu, Carlos
A. Murillo, Boris S. Tsukerblat, Dino Villagrn, and Xiaoping Wang

J. Am. Chem. Soc., **2005**, 127 (13), 4895-4902• DOI: 10.1021/ja044185b • Publication Date (Web): 10 March 2005

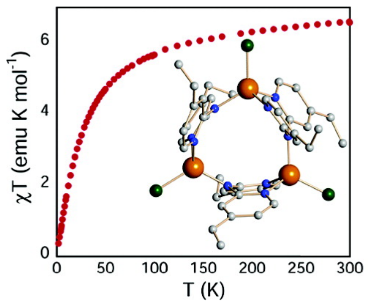

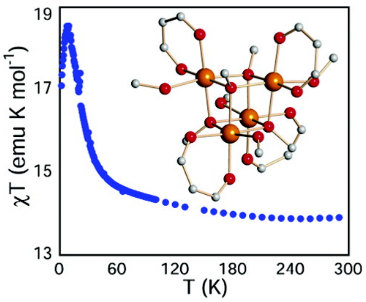

Journal of the American Chemical Society is published by the American Chemical Society. 1155 Sixteenth Street N.W., Washington, DC 20036

J|A|C|S
ARTICLES

Modeling Spin Interactions in a Cyclic Trimer and a Cuboidal Co_4O_4 Core with Co(II) in Tetrahedral and Octahedral Environments

John F. Berry,[†] F. Albert Cotton,*[,†] Chun Y. Liu,[†] Tongbu Lu,[†,§] Carlos A. Murillo,*[,†]
Boris S. Tsukerblat,*[,‡] Dino Villagrán,[†] and Xiaoping Wang[†]

Contribution from the Department of Chemistry and Laboratory for Molecular Structure and Bonding, P.O. Box 30012, Texas A&M University, College Station, Texas 77842-3012, Department of Chemistry, Ben-Gurion University of the Negev, P.O. Box 653, Beer-Sheva 84105, Israel, and School of Chemistry & Chemical Engineering, Sun-Yat Sen University, Guangzhou 510275, P. R. China

Received September 24, 2004; E-mail: cotton@tamu.edu; murillo@tamu.edu; tsuker@bgumail.bgu.ac.il

Abstract: The X-ray crystallographic structures, the magnetic susceptibilities from 2 to 300 K, and a theoretical analysis of the magnetism for a triangular and a tetranuclear molecule consisting of linked high-spin cobalt(II) centers are described. The interpretation of the magnetic data for the triangular compound $[Co(depa)Cl]_3$ (depa is the anion of 2,2′-(bis-4-ethylpyridyl)amine), which has tetrahedrally coordinated Co^{2+} ions, entails isotropic antiferromagnetic exchange interaction and antisymmetric exchange acting within the two low-lying spin doublets. Two strong isotropic ferromagnetic interactions have been modeled in the cuboidal compound $Co_4(DPM)_4(CH_3O)_4(CH_3OH)_4$ **(**DPM represents the anion of dipivaloylmethane), which has octahedral coordination, and the system can be approximately considered as two weakly coupled $S = 3$ species.

Introduction

The discovery of the single molecular magnetism phenomenon[1] has created a strong impetus for the study of the exchange interactions in clusters with a large number of coupled paramagnetic centers, such as the so-called Mn_{12} cluster ($Mn_{12}O_{12}(OAc)_{16}(H_2O)_4$).[1d,e] In the past few years there has been also renewed interest in smaller metal clusters, like triangular systems[2] in which interplay between isotropic and anisotropic exchange interactions[3] gives rise to a number of interesting peculiarities in the magnetic properties, including EPR. These relatively simple systems are helpful for testing models of exchange interaction and provide a good basis for the study of the magnetic anisotropy. Examples are the studies of associated Co(II) atoms joined by appropriate linkers giving dinuclear,[4] tetranuclear,[5] and larger clusters[6] in which there may be ferromagnetic or antiferromagnetic coupling between cobalt atoms.

However, it should be kept in mind that the magnetic behavior of high-spin cobalt(II) complexes has long been known to provide many traps for the unwary because of the great variety of magnetic behaviors they exhibit depending on factors such as the type and number of ligands that can give rise to low-[7] or high-spin[8] tetrahedral or octahedral complexes or those with other geometries.[9] Even for a given geometry such as in the tetrahedral $CoCl_4^{2-}$ ions, commonly found distortions have

---

[†] Texas A&M University.

[‡] Ben-Gurion University of the Negev.

[§] Sun-Yat Sen University.

(1) (a) Gatteschi, D.; Sessoli, R. *Angew. Chem., Int. Ed.* **2003**, *42*, 268. (b) Christou, G.; Gatteschi, D.; Hendrickson, D. N.; Sessoli, R. *MRS Bull.* **2000**, *25*, 66. (c) Awschalom, D. D.; Di Vencenzo, D. P. *Phys. Today* **1995**, 43. (d) Sessoli, R.; Tsai, H.-L.; Schake, A. R.; Wang, S.; Vincent, J. B.; Folting, K.; Gatteschi, D.; Christou, G.; Hendrickson, D. N. *J. Am. Chem. Soc.* **1993**, *115*, 1804. (e) Sessoli, R.; Gatteschi, D.; Caneschi, A.; Novak, M. A. *Nature* **1993**, *365*, 141. (f) Schelter, E. J.; Prosvirin, A. V.; Dunbar, K. R. *J. Am. Chem. Soc.* **2004**, *126*, 15004.

(2) (a) Gatteschi, D.; Sessoli, R.; Plass, W.; Müller, A.; Krickemeyer, E.; Meyer, J.; Sölter, D.; Adler, P. *Inorg. Chem.* **1996**, *35*, 1926. (b) Ferrer, S.; Lloret, F.; Bertomeu, I.; Alzuet, G.; Borrás, J.; García-Granda, S.; Liu-González, M.; Haasnoot, J. G. *Inorg. Chem.* **2002**, *41*, 5821. (c) Liu, X.; de Miranda, M. P.; McInnes, E. J. L.; Kilner, C. A.; Halcrow, M. A. *Dalton Trans.* **2004**, 59. (d) Glaser, T.; Heidemeier, M.; Grimme, S.; Bill, E. *Inorg. Chem.* **2004**, *43*, 5192. (e) Cage, B.; Cotton, F. A.; Dalal, N. S.; Hillard, E. A.; Ravkin, B.; Ramsey, C. M. *J. Am. Chem. Soc.* **2003**, *125*, 5270. (f) Cage, B.; Cotton, F. A.; Dalal, N. S.; Hillard, E. A.; Ravkin, B.; Ramsey, C. M. *C. R. Chimie* **2003**, *6*, 39. (g) Belinsky, M. I. *Inorg. Chem.* **2004**, *43*, 739. (h) Tsukerblat, B. S.; Palii, A. V.; Mirovitskii , V. Yu.; Ostrovsky, S. M.; Turta, K.; Jovmir, T.; Shova, S.; Bartolome, J.; Evangelisti, M.; Filoti, G. *J. Chem. Phys.* **2001**, *115*, 9528. (i) Yoon, J.; Mirica, L. M.; Stack, T. D. P.; Solomon, E. I. *J. Am. Chem. Soc.* **2004**, *126*, 12586.

(3) (a) Tsukerblat, B. S.; Belinskii, M. I.; Fainzilberg, V. E. Magnetochemistry and Spectroscopy of Transition Metal Exchange Clusters. In *Soviet Science Review B*; Vol'pin, M. E., Ed.; Harwood Academic Publishers: New York, 1987; Vol. 9, pp 337−482. (b) Tsukerblat, B. S.; Belinskii, M. I. *Magnetochemistry and Radiospectroscopy of Exchange Clusters*; Shtiintsa Publishers: Kishinev, 1983 (in Russian).

(4) (a) Lasarov, N. D.; Spasojevic, V.; Kusigerski, V.; Matic, V. M.; Milic, M. *J. Magn. Magn. Mater.* **2004**, *272*, 1065. (b) Sakiyama, H.; Ito, R.; Kumagai, H.; Inoue, K.; Sakamoto, M.; Nishida, Y.; Yamasaki, M. *Eur. J. Inorg. Chem.* **2001**, 2027. (c) Hossain, M. J.; Yamasaki, M.; Mikuyira, M.; Kuribayashi, A.; Sakiyama, H. *Inorg. Chem.* **2002**, *41*, 4058.

(5) (a) Tsohos, A.; Dionyssopoulou, S.; Raptopoulou, C. P.; Terzis, A.; Bakalbassis, E. G.; Perlepes, S. P. *Angew. Chem., Int. Ed.* **1999**, *38*, 983. (b) Bertrand, J. A.; Ginsberg, A. P.; Kaplan, R. I.; Kirkwood, C. E.; Martin, R. L.; Sherwood, R. C. *Inorg. Chem.* **1971**, *10*, 240. (c) Seisenbaeva, G. A.; Kritikos, M.; Kessler, V. G. *Polyhedron* **2003**, *22*, 2581. (d) Galán-Mascarós, J. R.; Dunbar, K. R. *Chem. Commun.* **2001**, 217.

(6) See for example: Brechin, E. K.; Cador, O.; Caneschi, A.; Cadiou, C.; Harris, S. G.; Parsons, S.; Vonci, M.; Winpenny, R. E. P. *Chem. Commun.* **2002**, 1860.

(7) Jenkins, D. M.; Di Bilio, A. J.; Allen, M. J.; Betley, T. A.; Peters, J. C. *J. Am. Chem. Soc.* **2002**, *124*, 15336.

10.1021/ja044185b CCC: $30.25 © 2005 American Chemical Society

important effects on the magnetic behavior because of zero-field splitting.[10] This is true for both tetrahedral and octahedral complexes, but when the symmetry is less than cubic, either by distortions of these idealized polyhedra or when the coordination number is 5, the complexities of the theory increase even more. When several cobalt(II) ions are magnetically coupled to each other, as in polynuclear complexes, it can be very challenging to obtain a close and meaningful fit to the experimentally measured magnetic data because magnetic coupling and zero-field splitting effects, which often work in concert, tend to be nearly impossible to deconvolute.

In this paper we report two new polynuclear molecules consisting of linked high-spin cobalt(II) centers. One compound, $[Co(depa)Cl]_3$ (**1**), contains three cobalt(II) ions, each tetrahedrally coordinated, that lie at the vertices of an equilateral triangle. Here depa, **I**, is the anion of 2,2′-(bis-4-ethylpyridyl)-amine. The other compound, $Co_4(DPM)_4(CH_3O)_4(CH_3OH)_4$ (**2**), has a cuboidal Co_4O_4 core with each cobalt(II) ion octahedrally coordinated, and DPM, **II**, represents the anion of dipivaloylmethane.

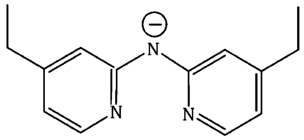

I

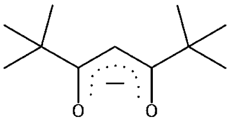

II

For each compound we describe in detail the structure, based on X-ray crystallography, the bulk magnetic susceptibility from 2 to 300 K, and a theoretical analysis of the magnetism that leads to a good fitting of the experimental data based on a rational model. Analysis of the magnetic behavior of **1** requires attention to the *spin frustration* problem imposed by the triangular structure. The spin frustration is closely related to the symmetry of the spin system and is affected by orbital degeneracy arising from the exchange interaction between magnetic ions. For example, in rigorously triangular systems with half-integer spins, the ground state can be represented as the orbital doublet ^2E. In such systems the antisymmetric exchange (AS) term becomes important and leads to a specific zero-field splitting and magnetic anisotropy due to orbital contributions to the magnetic exchange.[3] In compound **1** the isotropic magnetic coupling is antiferromagnetic and results in a limiting low-temperature moment corresponding to $S = {}^1/_2$. The dominant magnetic interactions in **2** are ferromagnetic.

Experimental Section

General. All manipulations were carried out under an atmosphere of nitrogen gas using standard Schlenk techniques, unless specified otherwise. Solvents were distilled over appropriate drying agents under a nitrogen atmosphere; 2,2′-bis-4,4′-ethylpyridylamine (Hdepa) was synthesized according to a published procedure.[11] Cobalt dichloride was purchased from Strem Chemicals and heated in refluxing thionyl chloride prior to use, and $Co(DPM)_2$ was prepared by following a published method.[12]

Physical Measurements. The IR spectra were taken on a Perkin-Elmer 16PC FTIR spectrometer for **1** and on a Bruker Tensor 27 spectrometer for **2** using KBr pellets. Electronic spectra were measured on a SHIMADZU UV-2501PC spectrophotometer. Elemental analyses were carried out by Canadian Microanalytical Services in British Columbia, Canada. Variable-temperature magnetic susceptibility measurements were made on crushed crystalline samples. Each sample was carefully weighed and placed in a plastic bag, which was mounted in a drinking straw and then placed inside a Quantum Design SQUID magnetometer MPMS-XL. Data were collected from 2 to 300 K at a field of 1000 G, and the data were corrected empirically for diamagnetism of the sample and the holder. Magnetization data for **2** were obtained at a constant temperature of 2 K using magnetic fields ranging from 0 to 7 T.

Preparation of $[Co(depa)Cl]_3$, 1. Hdepa (0.454 g, 2.00 mmol) was dissolved in 20 mL of THF. The solution was cooled with dry ice, and 1.3 mL of 1.6 M CH_3Li (2.08 mmol) was added slowly. The solution was allowed to warm to room temperature, and the yellow solution was then transferred via cannula to a reaction flask containing anhydrous $CoCl_2$ (0.260 g, 2.00 mmol). The mixture was stirred at room temperature for 1 h and then refluxed for 16 h, giving a deep green-brown solution. After addition of hexanes (30 mL) a precipitate formed, which was filtered off and washed with hexanes. The solid was then extracted with CH_2Cl_2 (2 × 10 mL), and the solution was then layered with hexanes. After 2 weeks, large deep-blue crystals of $[Co(depa)Cl]_3$, together with some greenish crystals of $Co(Hdepa)Cl_2$,[13] had formed. They were separated manually, and the blue crystals were washed with hexanes and dried under vacuum. Yield: 0.15 g, 23%. Anal. Calcd for $Co_3C_{42}H_{48}N_9Cl_3$: C, 52.44; H, 4.99; N, 13.10. Found: C, 52.38; H, 4.92; N, 13.07. IR (KBr, cm^{-1}): 3754 w, 3426 m, 2969 m, 1613 s, 1544 m, 1421 vs, 1346 m, 1275 w, 1227 m, 1183 m, 1059 w, 1020 m, 904 m, 828 m, 659 w, 552 w, 478 w. Vis (λ_{max}, nm (ϵ, M^{-1} cm^{-1})): 610 (1000), 536 (1000), 522 (900).

Preparation of $Co_4(DPM)_4(CH_3O)_4(CH_3OH)_4$, 2. Crystalline $Co(DPM)_2$ (2.50 g, 5.88 mmol) was dissolved in 10 mL of CH_2Cl_2. The resultant red solution was layered with 45 mL of CH_3OH. Large red crystals of **2** were obtained after 2 days of diffusion. Yield: 1.45 g, 82%. Anal. Calcd for $C_{52}H_{104}Co_4O_{16}$: C, 51.15; H, 8.50. Found: C, 50.88; H, 8.55. IR (KBr, cm^{-1}): 2963 s, 2869 m, 1569 s, 1504 s, 1388 s, 1246 m, 1183 m, 871 m, 763 m. Vis (λ_{max}, nm (ϵ, M^{-1} cm^{-1})): 443 (44), 549 (144).

X-ray Crystallography. Single crystals of **1** and **2** were each mounted and centered in the goniometer of a Bruker SMART 1000 CCD area detector diffractometer and cooled to −60 °C. Geometric and intensity data were collected using SMART software.[14] Data were processed using SAINT software,[15] and corrections for absorption were

---

(8) (a) Cotton, F. A.; Goodgame, M. *J. Am. Chem. Soc.* **1961**, *83*, 1777. (b) Cotton, F. A.; Faut, O. D.; Goodgame, D. M. L.; Holm, R. H. *J. Am. Chem. Soc.* **1961**, *83*, 1780. (c) Cotton, F. A.; Goodgame, D. M. L.; Goodgame, M. *J. Am. Chem. Soc.* **1961**, *83*, 4690. (d) Davies, J. E.; Gerloch, M.; Phillips, D. J. *J. Chem. Soc., Dalton Trans.* **1979**, 1836. (e) Romerosa, A.; Saraiba-Bello, C.; Serrano-Ruiz, M.; Caneschi, A.; McKee, V.; Peruzzini, M.; Sorace, L.; Zanobini, F. *Dalton Trans.* **2003**, 3233.

(9) Cotton, F. A.; Wilkinson, G.; Murillo, C. A.; Bochmann, M. *Advanced Inorganic Chemistry*, 6th ed.; John Wiley & Sons: New York, 1999.

(10) Carlin, R. L. *Science* **1985**, *227*, 1291.

(11) Berry, J. F.; Cotton, F. A.; Lu, T.; Murillo, C. A.; Wang, X. *Inorg. Chem.* **2003**, *42*, 3595.

(12) Cotton, F. A.; Liu, C. Y.; Murillo, C. A.; Wang, X. *Inorg. Chem.* **2003**, *42*, 4619.

(13) Crystal data for $CoC_{14}H_{17}N_3Cl_2$ ($Co(Hdepa)Cl_2$): orthorhombic, *Pbca*, $a = 14.6284(11)$ Å, $b = 14.1360(11)$ Å, $c = 15.2538(12)$ Å, $V = 3154.3(4)$ Å^3, $d = 1.419$ g cm^{-3}, R1 ($I > 2F(I)$) = 0.0264, wR2 ($I > 2\sigma(I)$) = 0.0694, R1 (all data) = 0.0328, wR2 (all data) = 0.0750. Important bond distances: Co1−N1 = 2.006(1), Co1−N3 = 1.999(1), Co1−Cl1 = 2.2191(5), Co1−Cl2 = 2.2473(5). Relevant bond angles: N1−Co1−N3 = 94.02(5), N1−Co1−Cl1 = 113.11(4), N1−Co1−Cl2 = 110.02(4), N3−Co1−Cl1 = 116.01(4), N3−Co1−Cl2 = 108.23(4), Cl1−Co1−Cl2 = 113.73(2). These structural parameters are similar to those in the ethyl-free analogue $Co(Hdpa)Cl_2$. See: Cotton, F. A.; Daniels, L. M.; Jordan, G. T., IV; Murillo, C. A. *Polyhedron* **1998**, *17*, 589.

(14) *SMART V5.618, Program for Data Collection on Area Detectors*; Bruker AXS Inc., 5465 East Cheryl Parkway, Madison, WI 53711-5373.

(15) *SAINTPLUS V6.45, Program for Reduction of Area Detector Data*; Bruker AXS Inc., 5465 East Cheryl Parkway, Madison, WI 53711-5373.

Chart 1

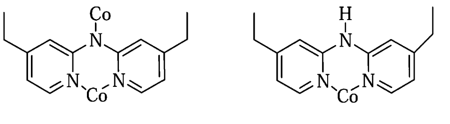

III **IV**

applied using the program SADABS.[16] The structures were solved via the direct methods program in the SHELXTL software package.[17] Least-squares refinement followed by difference Fourier synthesis revealed the positions of all non-hydrogen atoms. Hydrogen atoms were placed in calculated positions using a riding model for the last refinement cycle. Table S1 summarizes the refinement details for **1** and **2**. Tables S2 and S3 provide the main structural information for **1** and **2**, respectively. A displacement ellipsoid plot of Co(Hdepa)Cl_2 is given as Supporting Information.

Results and Discussion

Syntheses. The deep-blue compound **1** was synthesized in a straightforward manner by reaction of anhydrous $CoCl_2$ and Lidepa in a 1:1 ratio:

$$3\mathrm{CoCl_2} + 3\mathrm{Lidepa} \rightarrow [\mathrm{Co(depa)Cl}]_3 + 3\mathrm{LiCl}$$

A byproduct,[13] Co(Hdepa)Cl_2, which is greenish blue, was often present and appears to form as a consequence of incomplete deprotonation of the Hdepa ligand during the preparation of Lidepa. The crystals can be easily separated manually.

Compound **2** was readily prepared by alcoholysis of the β-diketonate derivative $Co(DPM)_2$ under ambient conditions. The tetramerization of the mononuclear complex in the presence of methanol is an essentially quantitative process, and can be described by the equation:

$$4\mathrm{Co(DPM)_2} + 8\mathrm{CH_3OH} \rightarrow \mathrm{Co_4(DPM)_4(CH_3O)_4(CH_3OH)_4} + 4\mathrm{HDPM}$$

The low solubility of **2** in methanol appears to be the driving force for the reaction. The ready formation of the cluster is attributable to the choice of the precursor. The tetrahedral complex $Co(DPM)_2$ can be prepared in good yield by direct synthesis from a source of Co(II) ions and HDPM. It is to be noted that cobalt(II) and nickel(II) acetylacetonate analogues were prepared decades ago using the corresponding mononuclear complexes $M(acac)_2$,[18,5b] but for these compounds harsher reaction conditions, such as addition of base and elevated temperature, were employed.

Structures. Both **1** and the blue-green byproduct feature Co^{2+} ions in a tetrahedral geometry, with a chelating coordination mode of the Hdepa ligands. In the byproduct the Hdepa ligand is still protonated, so the complex remains mononuclear. In **1**, the depa ligand which is a monoanion uses the third exposed N atom to bridge to another Co atom. This is shown schematically as **III** in Chart 1, along with the more usual binding mode, **IV**, found in Co(Hdepa)Cl_2. It should be noted that the depa ligand can also form complexes with a linear arrangement of three Co atoms in a triply bridging coordination mode.[19] In both of these complexes, the coordination sphere around each Co atom is significantly distorted from the ideal tetrahedral arrangement. In Co(Hdepa)Cl_2, the N−Co−N angle of 94° is much smaller than the other angles, presumably because of the bite of the chelating ligand. In **1**, the chelating N−Co−N angles of ∼91° are also smaller than the other angles, which range from 108° to 120°. As shown in Figure 1, the three Co(II) units form a triangle with idealized C_{3h} symmetry in which all of the Co−N and Co−Cl distances are normal (Table 1).

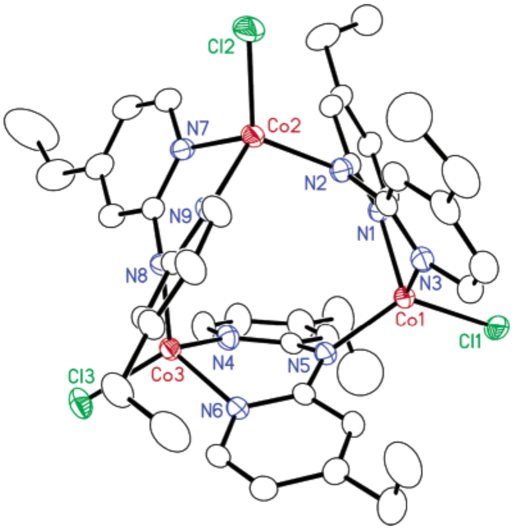

Figure 1. Thermal ellipsoid plot of the cyclic trimer **1** with ellipsoids drawn at the 30% probability level and hydrogen atoms removed.

Table 1. Selected Bond Distances (Å) and Angles (°) for **1** and **2**

1		**2**	
Co−N (av)	1.997(9)	Co−O_{MeO}(av)	2.09(2)
Co−Cl (av)	2.235(3)	Co−O_{MeOH}(av)	2.19(1)
N−Co−N (av)[a]	110(2)	O−Co−O (av)[c]	82(1)
N−Co−N (av)[b]	91.3(4)	O−Co−O (av)[d]	87.2(3)
N−Co−Cl (av)	114(5)	Co−O−Co (av)[e]	97(2)

[a] The two nitrogen atoms belong to two different ligands, e.g., N(1)−Co(1)−N(5). [b] The two nitrogen atoms belong to the same ligand, e.g. N(1)−Co(1)−N(3). [c] Angles for the Co_4O_4 core. [d] Oxygen atoms from DPM ligand. [e] Of the six faces of the cube, two opposite faces have Co−O−Co angles of ca. 99°, while in the other four, these angles are ca. 96°.

The overall structure of **2** (Figure 2) is tetranuclear, and it has a cuboidal Co_4O_4 core with the four octahedrally coordinated cobalt(II) atoms occupying four alternating corners of a cube. The other corners are occupied by oxygen atoms of methoxide groups. The overall arrangement has idealized S_4 symmetry. This arrangement and symmetry of metal and bridging atoms have been seen in other tetranuclear clusters such as Fe_4S_4,[20] Fe_4O_4,[21] Mn_4O_4,[21b,22] and Ni_4O_4.[5b] To furnish a complete octahedral coordination environment, each cobalt ion is also bonded to a CH_3OH molecule and chelated by a β-diketonate ligand (DPM).

---

(16) *SADABS V2.10, Program for Absorption Correction of Area Detector Frames*; Bruker AXS Inc., 5465 East Cheryl Parkway, Madison, WI 53711-5373.

(17) *SHELXTL V6.12*; Bruker AXS Inc., 5465 East Cheryl Parkway, Madison, WI 53711-5373.

(18) Bertrand, J. A.; Caine, D. *J. Am. Chem. Soc.* **1964**, *86*, 2298.

(19) Berry, J. F.; Cotton, F. A.; Lu, T.; Murillo, C. A. *Inorg. Chem.* **2003**, *42*, 4425.

(20) (a) Holm, R. H. Iron−Sulfur Clusters. In *Comprehensive Coordination Chemistry II*; Elsevier: New York, 2003; Vol. 8, Section 83, p 6190. (b) Zhou, H.-C.; Holm, R. H. *Inorg. Chem.* **2003**, *42*, 11. (c) Davies, S. C.; Evans, D. J.; Henderson, R. A.; Hughes, D. L.; Longhurst, S. *J. Chem. Soc., Dalton Trans.* **2001**, 3470. (d) Gloux, J.; Gloux, P.; Laugier, J. *J. Am. Chem. Soc.* **1996**, *118*, 11644.

(21) See for example: (a) Clemente-Juan, J. M.; Mackiewicz, C.; Verelst, M.; Dahan, F.; Bousseksou, A.; Sanakis, Y.; Tuchagues, J.-P. *Inorg. Chem.* **2002**, *41*, 1478. (b) Taft, K. L.; Caneschi, A.; Pence, L. E.; Delfs, C. D.; Papaefthymiou, G. C.; Lippard, S. J. *J. Am. Chem. Soc.* **1993**, *115*, 11753.

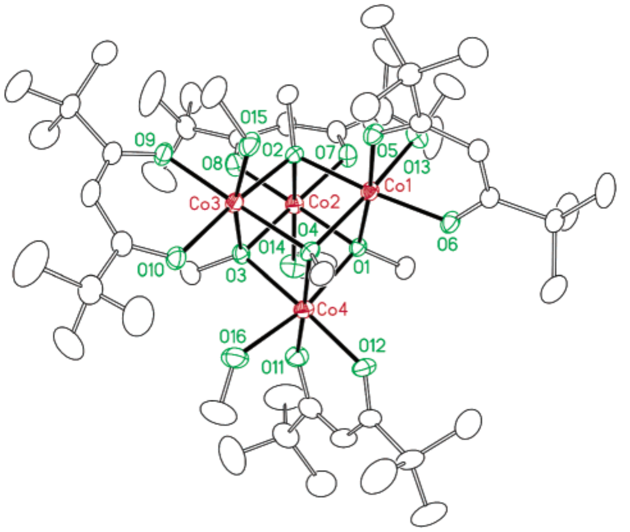

Figure 2. Thermal ellipsoid plot of **2** drawn at the 30% probability level and hydrogen atoms removed.

Chart 2[a]

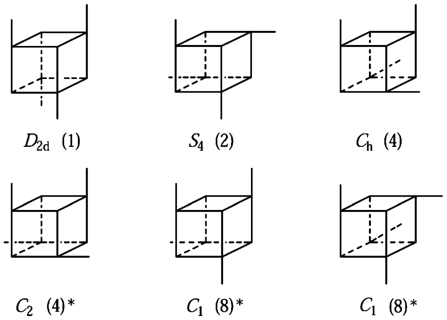

[a] Asterisk indicates half are enantiomers of the other half.

The cuboidal core is distorted, with all the O−Co−O angles being smaller than 90°, while all the Co−O−Co angles are larger than 90°. Similarly to the acac analogue,[5b] the Co···Co separations vary from 3.095 to 3.197 Å.

There are many possible isomers for this molecule, but only one was observed. Since there are three directions for the M−O bonds to the four-coordinated methanol molecules, one can easily (although tediously) list $3^4 = 81$ permutations. This number may be immediately reduced to 27 by noting that these may be sorted into three equivalent sets, each arising from the choice of orientation made at whatever metal atom is chosen as the first. For example, if xxxx represents the isomer with all four M−O bonds lying parallel to the X direction, xxxy and xxxz are the isomers with three M−O bonds parallel to the *X* axis and the fourth one parallel to the *Y* or *Z* direction, and so on.

Further analysis shows that among the 27 distinct permutations mentioned above there are only six discrete geometric isomers. These are presented in Chart 2. For each one we note the point symmetry followed by the number of those in the list of 27 that are actually identical or enantiomers. In the last three cases, where there is only C_2 symmetry or no symmetry, the isomers occur in enantiomeric pairs. Compound **2** has a structure that belongs to the second group which has S_4 symmetry.

Magnetic Properties. The ground state of a Co^{2+} ion (d^7) in a tetrahedral surrounding is $^4A_2$, $S = {}^3/_2$, and thus the orbital angular momentum contribution is a second-order effect. Under this condition the Heisenberg−Dirac−Van Vleck (HDVV) isotropic exchange model can be employed in compound **1**. Because of the triangular structure of the Co^{2+} trimer, we use the geometry of an equilateral triangle where the HDVV Hamiltonian takes the form:

$$\mathscr{H}_1 = -2J(\boldsymbol{S}_1\boldsymbol{S}_2 + \boldsymbol{S}_1\boldsymbol{S}_3 + \boldsymbol{S}_2\boldsymbol{S}_3) \tag{1}$$

in which *J* is the exchange parameter, $S_1 = S_2 = S_3 = {}^3/_2$, and the eigenvalues are

$$E(S) = -J[S(S+1) - 45/4] \tag{2}$$

The eigenvectors $|(S_{12})SM\rangle$ of the Hamiltonian in eq 1 are specified also by the intermediate spin S_{12} in the vector coupling scheme for three spins: $S_1 + S_2 = S_{12}$, $S_{12} + S_3 = S$. The $(S_{12})S$ states are degenerate with respect to S_{12}, which can be indicated as (1,2) $^1/_2$, (0,1,2,3) $^3/_2$, (1,2,3) $^5/_2$, (2,3) $^7/_2$, (3) $^9/_2$. This additional degeneracy, conventionally called "accidental degeneracy", is a result of the unitary symmetry of the HDVV Hamiltonian and, in particular, it is related to the orbital degeneracy of the HDVV multiplets.[3] It should be emphasized that there are two spin-doublet states, $(S_{12})S =$ (1) $^1/_2$ and (2) $^1/_2$, so that the ground state proves to be four-fold degenerate and can be associated with the orbital doublet ^2E in C_{3v}. The term ^2E is split into two Kramers doublets by spin−orbit interaction that can be introduced in the spin-coupling scheme by inclusion of the antisymmetric (AS) exchange term (Dzyaloshinsky−Moria interaction[23]):

$$\mathscr{H}_{AS} = \sum_{i,j} \boldsymbol{G}_{ij}[\boldsymbol{S}_i \times \boldsymbol{S}_j] \tag{3}$$

where $[\boldsymbol{S}_i \times \boldsymbol{S}_j]$ is the vector product, and the antisymmetric vector parameters $G_{ij} = -G_{ji}$ are proportional to the spin−orbit coupling parameter. The gap between Kramers doublets proves to be $2|G|$, with $G \equiv G_Z$ being the collective AS exchange parameter relating to the pairwise interactions G^z_{12}, G^z_{23}, and G^z_{31} by the relation[3] $G = (2/\sqrt{3})(G^z_{12} + G^z_{13} + G^z_{23})$. For trigonal symmetry, G_X and G_Y vanish so that the vector *G* is parallel to the C_3 axis, thus reflecting the axial magnetic symmetry. As distinguished from the HDVV interaction, the AS exchange introduces magnetic anisotropy in trimeric systems.[24] According to the symmetry of the system, the Hamiltonian of the Zeeman interaction is assumed to be axial with $g_{\|}$ and $g_{\perp}$:

$$\mathscr{H}_Z = g_{\|}\beta S_Z H_Z + g_{\perp}\beta(S_X H_X + S_Y H_Y) \tag{4}$$

We shall consider a relatively simple model including the joint effect of AS exchange and Zeeman interaction within the two low-lying spin-doublets (1) $^1/_2$, (2) $^1/_2$. The next order

---

(22) (a) Pence, L. E.; Caneschi, A.; Lippard, S. J. *Inorg. Chem*. **1996**, *35*, 3069. (b) McKee, V.; Shepard, W. B. *J. Chem. Soc., Chem. Commun*. **1985**, 158. (c) Brooker, S.; McKee, V.; Shepard, W. B.; Pannell, L. K. *J. Chem. Soc., Dalton Trans*. **1987**, 2555.

(23) (a) Dzyaloshinsky, I. *Phys. Chem. Solids* **1958**, *4*, 241. (b) Dzyaloshinsky, I. *Sov. Phys.-JETP* **1958**, *6*, 1130. (c) Moria, T. *Phys. Rev.* **1960**, *117*, 635. (d) Moria, T. *Phys. Rev.* **1960**, *120*, 91.

(24) (a) Belinsky, M. I.; Tsukerblat, B. S.; Ablov, A. V. *Fiz. Tverd. Tela (Sov.)* **1974**, *16*, 989. (b) Belinsky, M. I.; Tsukerblat, B. S.; Ablov, A. V. *Mol. Phys.* **1974**, *28*, 283. (c) Tsukerblat, B. S.; Kyavskaya, B. Ya.; Belinsky, M. I.; Ablov, A. V.; Novotortsev, V. M.; Kalinnikov, V. T. *Theor. Chim. Acta* **1975**, *38*, 131. (d) Tsukerblat, B. S.; Kyavskaya, B. Ya.; Belinsky, M. I.; Ablov, A. V.; Novotortsev, V. M.; Kalinnikov, V. T. *Pis'ma Zh. Teor. Exp. Fiz.* **1975**, *19*, 525. (f) See also ref 3a.

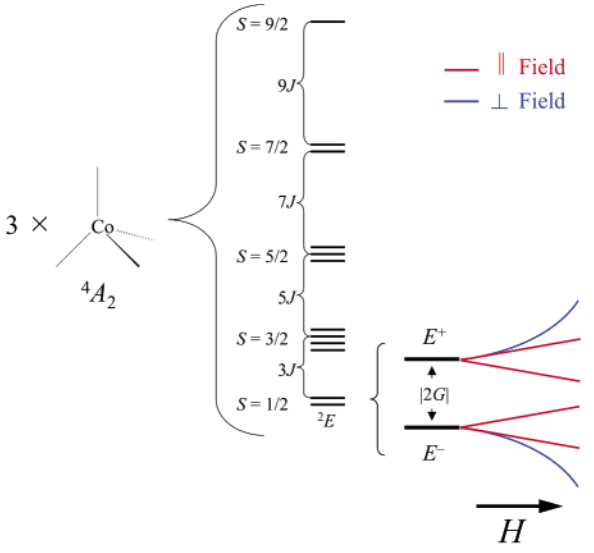

Figure 3. Schematic representation of the states arising from three tetrahedral cobalt centers coupled to each other in **1**. At the right of the scheme, the zero-field splitting due to AS exchange is shown along with the angular field dependence.

perturbation including mixing with the excited spin levels will be neglected as well as the splitting of these levels. The matrix elements of $\mathscr{H}_{\mathrm{AS}} + \mathscr{H}_Z$ are calculated using the irreducible tensor operator technique,[3b,25] the resulting 4 × 4 matrix can be solved in analytical form, and the energies of the magnetic sublevels are given by

$$\begin{aligned} E^{+}_{1,2} &= \frac{1}{2}\sqrt{(2G \pm g_{\|}\beta H \cos\vartheta)^2 + g_{\perp}^2\beta^2H^2\sin^2\vartheta} \\ E^{-}_{1,2} &= -\frac{1}{2}\sqrt{(2G \pm g_{\|}\beta H \cos\vartheta)^2 + g_{\perp}^2\beta^2H^2\sin^2\vartheta} \end{aligned} \quad (5)$$

In eq 5, $E^{+}_{1,2}$ and $E^{-}_{1,2}$ are related to two Kramers doublets (separated by the gap $2|G|$ at $H = 0$), the symbols 1 and 2 enumerate Zeeman sublevels associated with these doublets, and ϑ is the angle between the field and the C_3 axis of the system. The interplay between AS exchange and the anisotropic contributions to g factors of Co^{2+} ions determines the magnetic anisotropy of the entire trimer. This can be clearly demonstrated by consideration of the low-field behavior of the magnetic sublevels that can be found from the general expressions eq 5. With an accuracy to $(\beta H/G)^2$ one obtains

$$\begin{aligned} E^{+}_{1,2} &= G \pm \frac{1}{2}g_{\|}\beta H\cos\vartheta + \frac{g_{\perp}^2\beta^2H^2}{8G}\sin^2\vartheta \\ E^{-}_{1,2} &= -G \mp \frac{1}{2}g_{\|}\beta H\cos\vartheta - \frac{g_{\perp}^{2}\beta^2H^2}{8G}\sin^2\vartheta \end{aligned} \quad (6)$$

One can see that in a parallel field ($\vartheta = 0$) the Kramers doublets are split and the sublevels vary linearly, $\pm g_{\|}\beta H/2$, with the field. Conversely, in a relatively weak ($(\beta H/G)^2 \ll 1$) perpendicular field, only quadratic terms, $g_{\perp}^2\beta^2H^2/8G$, appear so that the magnetic moment is reduced by the AS exchange. As a result of this effect, at low temperature, the system is expected to behave like a Van Vleck paramagnet. These effects are summarized in Figure 3, in which are shown all of the states arising from three tetrahedral cobalt centers coupled to each other. At the right of the figure, the zero-field splitting due to AS exchange is shown along with the angular field dependence.

Using conventionally accepted definitions,[26] one can find the temperature and field dependence of the molar magnetization (μ). The expressions for the parallel and perpendicular components are the following:

$$\begin{aligned} \mu_{\|}(H,T) = {} & \frac{1}{2}Ng_{\|}\beta\Big((8e^{3j}((2 + e^{12j})\sinh z + \\ & e^{5j}(3 + e^{16j})\sinh 2z + 3e^{12j}\sinh 3z + 2e^{21j}\sinh 4z))/ \\ & (2\cosh(G/kT) + 4e^{3j}(2 + e^{12j})\cosh z + 3e^{8j}(1 + \cosh 2z) + \\ & 4e^{15j}\cosh 3z + e^{24j}(1 + 2\cosh 2z + 4\cosh 4z))) + \\ & \tanh(z/2)\Big) \end{aligned} \quad (7)$$

$$\begin{aligned} \mu_{\perp}(H,T) = {} & Ng_{\perp}\beta(2g_{\perp}\beta H\sinh(\sqrt{4G^2 + g_{\perp}^2\beta^2H^2}/2kT) + \\ & e^{3j}((4 + 3e^{5j} + 2e^{12j} + e^{21j})\sinh(x/2) + 3(4 + 3e^{5j} + \\ & 2e^{12j} + e^{21j})\sinh(3x/2) + 5e^{5j}(3 + 2e^{7j} + 2e^{16j}) \times \\ & \sinh(5x/2) + 7e^{12j}(2 + e^{9j})\sinh(7x/2) + 9e^{21j} \times \\ & \sinh(9x/2))\sqrt{4G^2 + g_{\perp}^2\beta^2H^2})/(2(e^{3j}((4 + 3e^{5j} + 2e^{12j} + \\ & e^{21j})\cosh(x/2) + (4 + 3e^{5j} + 2e^{12j} + e^{21j})\cosh(3x/2) + \\ & e^{5j}(3 + 2e^{7j} + 2e^{16j})\cosh(5x/2) + e^{12j}(2 + e^{9j})\cosh(7x/2) + \\ & e^{21j}\cosh(9x/2)) + 2\cosh(\sqrt{4G^2 + g_{\perp}^2\beta^2H^2}/2kT)) \times \\ & \sqrt{4G^2 + g_{\perp}^2\beta^2H^2}) \end{aligned} \quad (8)$$

In eqs 7 and 8, β, N, and k have their usual meaning and the following dimensionless parameters are introduced: $j = J/kT$, $x = g_{\perp}\beta H/kT$, $z = g_{\|}\beta H/kT$. For the sake of simplicity we will give here the expressions for the main components of the magnetic susceptibility in the low-field limit:

$$\chi_{\|}(T) = \frac{Ng_{\|}^2\beta^2}{4kT} \times \frac{40e^{3j} + 105e^{8j} + 168e^{15j} + 165e^{24j} + 2\cosh(G/kT)}{8e^{3j} + 9e^{8j} + 8e^{15j} + 5e^{24j} + 2\cosh(G/kT)} \quad (9)$$

$$\chi_{\perp}(T) = \frac{Ng_{\perp}^2\beta^2}{4kT} \times \frac{40e^{3j} + 105e^{8j} + 168e^{15j} + 165e^{24j} + (2kT/G)\sinh(G/kT)}{8e^{3j} + 9e^{8j} + 8e^{15j} + 5e^{24j} + 2\cosh(G/kT)} \quad (10)$$

It should be noted that some anisotropic properties of the spin-frustrated ground state are affected by the AS exchange and this should be considered in the fitting. For the isolated ground manifold consisting of the two spin doublets with the energies given by eqs 5, one can find the following expression

---

[25] (a) Bencini, A.; Gattteschi, D. *Electron Paramagnetic Resonance of Exchange Coupled Systems*; Springer-Verlag: Berlin, 1990. (b) Gattteschi, D.; Pardi L. *Gazz. Chim. Ital.* **1993**, *123*, 231. (c) Tsukerblat, B. S. *Group Theory in Chemistry and Spectroscopy*; Academic Press: London, 1994. (d) Borrás-Almenar, J. J.; Clemente-Juan, J. M.; Coronado, E.; Tsukerblat, B. S. *Inorg. Chem.* **1999**, *38*, 6081.

[26] Kahn, O. *Molecular Magnetism*; Wiley-VCH: New York, 1993.

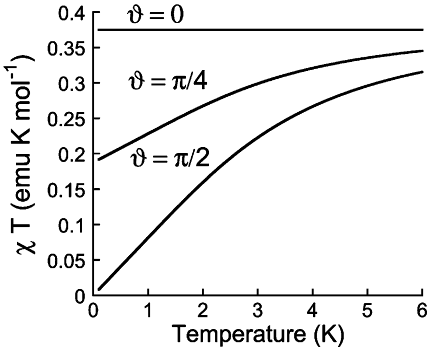

Figure 4. Influence of the AS exchange on the temperature dependence of χT for an idealized triangular trimer of Co^{2+} ions at different directions of the applied magnetic field with $g_\perp = g_\parallel = 2$ and $G = 3$ cm^{-1}; here θ denotes the angle between the C_3 axis and the magnetic field.

for χT in the low-field limit:

$$\chi T = \frac{N\beta^2}{4kG}\left[Gg_\parallel^2 \cos^2 \vartheta + kTg_\perp^2 \sin^2 \vartheta \tanh\frac{G}{kT}\right] \qquad (11)$$

In a parallel field one obtains $\chi_\parallel T = C_\parallel$, that is, the Curie law with the constant $C_\parallel = N\beta^2 g_\parallel^2/4k$. In the case of a perpendicular field we find $\chi_\perp T = [C_\perp kT/G][\tanh(G/kT)]$, with $C_\perp = N\beta^2 g_\perp^2/4k$, which is different from the Curie law. It should be noted that similar deviations from the Curie law have been observed for isotropic g-factors.[24] Figure 4 illustrates the dependence of χT vs T at different angles ϑ (for the sake of simplicity it is assumed that $g_\parallel = g_\perp = 2$) and it shows that the AS exchange strongly reduces χT, giving rise to the deviation from the Curie law when $\vartheta \neq 0$. This is one of the physical manifestations of spin frustration in an equilateral triangle of Co^{2+} ions that is inherently related to the orbital degeneracy of the ground state and, as a result, to a magnetic anisotropy implied by the AS exchange.

The experimental data on a powder sample of **1** were fitted using eqs 9 and 10 and the approximate expression for the susceptibility of a powder sample, $\chi = (\chi_\parallel + 2\chi_\perp)/3$. The fitting procedure and the derivation of eqs 5−11 were performed with the aid of *Mathematica-5*.[27] The magnetic behavior of the system is determined by four parameters: $g_\parallel$, $g_\perp$, G, and J. In order to reduce the excessive flexibility of the theoretical expressions and to avoid overparametrization, we performed a two-step fitting procedure. Because the high-temperature data are most sensitive to $g_\parallel$, $g_\perp$, and J, we fitted the data above 12 K assuming $G = 0$, and extracted G from the fit of the low-temperature data, which are most sensitive to the AS exchange and also influenced by the remaining interactions. Since it is evident from the general character of the experimental data that the HDVV interaction is antiferromagnetic, only negative J values were employed in the fitting. From Figure 5, one can see that the experimental data in the temperature range 2−300 K are perfectly reproduced by the theoretical curve. The resulting set of the best-fit parameters are the following: $J = -2.85(1)$ cm^{-1}, $G = 2.8(2)$ cm^{-1},[28] $g_\parallel = 2.7(4)$, $g_\perp = 1.96(27)$. The agreement factor, defined as $R = \sum_i[(\chi T)_i^{\text{exp}} - (\chi T)_i^{\text{calc}}]^2/\sum_i[(\chi T)_i^{\text{exp}}]^2$, is 4.8×10^{-5}. As far as the AS exchange acting within the ground manifold is concerned, the low-temperature behavior of χT vs T seems to be indicative. In the inset of Figure 5, this part of χT is shown separately along with the best-fit theoretical curve (lower) and the alternative theoretical dependence of χT vs T at $G = 0$ (upper). One can see that the low-temperature part is not adequately described by the isotropic model. It should be noted that the magnetic susceptibility at low temperatures favors the model that includes AS exchange. In fact, Figure 4 shows that $\chi_\perp T$ vanishes when $T \rightarrow 0$, so that χT vs T in a powder sample is not a constant at low temperatures as expected from the HDVV model. Unfortunately, experimental data at $T < 2K$ are not available.

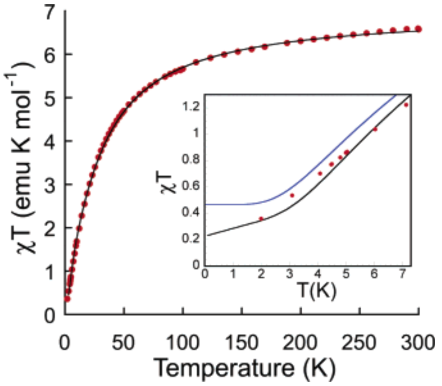

Figure 5. Plot of χT versus T for **1**. The solid black line is the theoretical fit of the data using the parameters given in the text. Inset: Low-temperature part of χT vs T dependence, lower curve corresponding to the best-fit parameters, upper curve in the isotropic model ($G = 0$, $J = -2.85$ cm^{-1}, $g_\parallel = 2.74$, $g_\perp = 1.96$).

Whereas the Co ions are linked by relatively weak isotropic antiferromagnetic interaction, the AS exchange is unexpectedly strong, as compared to the isotropic exchange. To make an approximate estimate of G, one can take into account that AS exchange appears as a second-order perturbation with respect to spin−orbit coupling and isotropic exchange connecting the ground states of two ions through the excited states. Accordingly to this mechanism, Moria[23c,d] proposed a semiquantitative estimate of a pairwise parameter of AS exchange, $G_{ij} \approx (\Delta g/g)\bar{J}$, where Δg is the anisotropic contribution to the g-factor and $\bar{J}$ is the HDVV parameter for the coupling between the ground state of the ion i and excited state of the ion j. Reliable information regarding the parameter $\bar{J}$ is unavailable. However, if values of $\Delta g \approx 0.7$ and $|\bar{J}| = 2.85$ are used, then G_{ij} is about 1 cm^{-1}, a value that is comparable to the isotropic exchange that results from strong anisotropy of the cobalt ions. Also, using the above-mentioned interrelation between G_{ij} and G, one can make a very rough estimate of $G = 3.2$ cm^{-1} for the AS exchange that, although high, is in reasonable agreement with the best-fit value. Halcrow et al.[2c] also came to the conclusion that $G_{ij} \approx (\Delta g/g)\bar{J}$ tends to underestimate the AS exchange parameter. It should be noted here that, since J and G appear to be of the same order of magnitude, it is possible that the perturbational treatment of this problem oversimplifies the matter. Other effects, such as state mixing, may also contribute to the observed magnetic phenomena, which have been neglected here. More rigorous methods, such as full-matrix diagonalization, may be necessary to more accurately determine the true values of J and G in this case. For the diferric

---

(27) Wolfram, S. *Mathematica-5*, version 5; Wolfram Research, Inc.: Champaign, IL, 2004 (see http://www.wolfram.com).

(28) It should be noted that the fit is not sensitive to the sign of the parameter G, and only the absolute value of G can be determined.

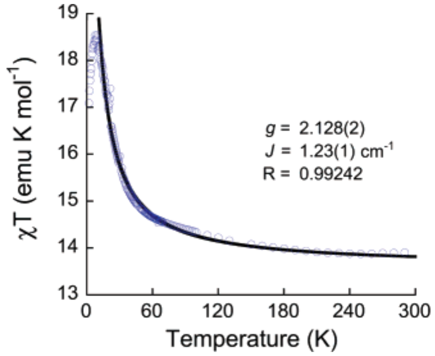

Figure 6. Plot of χT versus T for **2**. The solid line is the theoretical fit of the data using the parameters given in the inset. Data below 10 K were not fitted.

complexes, this kind of treatment has been given.[29] Also, more reliable information regarding the AS exchange could be extracted from the measurements that are directly related to the anisotropy of this kind of exchange, namely, the field and angular dependence of the magnetization at different temperatures and the angular dependence of EPR measured on single crystals.[3,2c] To conclude this discussion, it should be mentioned that the second-order terms with respect to spin−orbit coupling vanish within the basis of two spin-doublet states in a symmetric triangle, so the AS exchange is the only interaction that gives rise to a zero-field splitting.

For **2**, a consideration of the magnetic exchange interactions which can occur in an ideally cubic (T_d symmetry) Co_4O_4 system leads to the result that each face of the cube provides an exchange pathway between two Co atoms. This leads to the following Hamiltonian of the isotropic exchange interaction:[26]

$$\mathscr{H}_2 = -2J(\mathbf{S}_1\mathbf{S}_2 + \mathbf{S}_1\mathbf{S}_3 + \mathbf{S}_1\mathbf{S}_4 + \mathbf{S}_2\mathbf{S}_3 + \mathbf{S}_2\mathbf{S}_4 + \mathbf{S}_3\mathbf{S}_4) \tag{12}$$

A Jahn−Teller distortion of the four d^7 Co^{2+} ions lowers the symmetry of **1** to S_4 symmetry. This causes the six faces of the cube to have significantly different Co−O−Co angles. Two opposite faces have Co−O−Co angles of 99°, while the remaining four adjacent faces have average angles of 96°. Studies of compounds with planar hydroxo-bridged $Cu_2(OH)_2$ cores have shown that a change of ∼3° in the Cu−O−Cu angle can affect the coupling parameter J by as much as 200−300 cm^{-1}.[26] Thus, in the case of **2**, two J parameters are necessary to describe the interactions in the two different types of faces. For simplicity we will assume that $J > J'$ and thus obtain

$$\begin{aligned}\mathscr{H}_2^1 = {}& -2J(\mathbf{S}_1\mathbf{S}_2 + \mathbf{S}_3\mathbf{S}_4) - \\ & 2J'(\mathbf{S}_1\mathbf{S}_3 + \mathbf{S}_1\mathbf{S}_4 + \mathbf{S}_2\mathbf{S}_3 + \mathbf{S}_2\mathbf{S}_4) \\ = {}& -(J - J')(\mathbf{S}_{12}^2 + \mathbf{S}_{34}^2) - J'\mathbf{S}^2\end{aligned} \tag{13}$$

where $\mathbf{S}_{12} = \mathbf{S}_1 + \mathbf{S}_2$, $\mathbf{S}_{34} = \mathbf{S}_3 + \mathbf{S}_4$, and $\mathbf{S} = \mathbf{S}_{12} + \mathbf{S}_{34}$.

Since $S_1 = S_2 = S_3 = S_4 = 3/2$, a χT value of 7.5 emu K mol^{-1} is expected in the high-temperature limit. Surprisingly, the value measured is about twice as great. As shown in Figure 6, χT rises slowly from 14 emu K mol^{-1} with decreasing temperature, and below 50 K there is a steep increase to a maximum of 18.5 emu K mol^{-1} at 10 K. Further cooling to 2 K causes a sharp decrease in χT. From the value of the peak at 10 K, it appears that all four Co^{2+} ions are ferromagnetically coupled to give an $S = 6$ ground state.

The decrease in χT below 10 K is probably due to zero-field splitting,[30] and also due to the more common complications arising from spin−orbital interaction,[31] which as discussed earlier is a frequent source of difficulty in the interpretation of magnetic data for Co^{2+} complexes. The high-temperature value of $\chi T = 14$ emu K mol^{-1} is close to what is expected for a hypothetical molecule containing two $S = 3$ species. It therefore appears that one of the exchange constants, J, is so large that the Co^{2+} ions interacting through this pathway are ferromagnetically coupled at all temperatures measured. By letting $S_{12} = S_{34} = 3$, the zero-field Hamiltonian simplifies further to $H_2'' = -J'\mathbf{S}^2$.

Thus, $E(S) = -J'S(S + 1)$ and $E(0) = 0$, $E(1) = -2J'$, $E(2) = -6J'$, $E(3) = -12J'$, $E(4) = -20J'$, $E(5) = -30J'$, $E(6) = -42J'$.

From these energies, the following expression for the magnetic susceptibility can be derived:

$$\chi = \frac{Ng^2\beta^2}{3kT} \times \frac{6e^x + 30e^{3x} + 84e^{6x} + 180e^{10x} + 330e^{15x} + 546e^{21x}}{1 + 3e^x + 5e^{3x} + 7e^{6x} + 9e^{10x} + 11e^{15x} + 136e^{21x}} \tag{14}$$

where $x = 2J'/kT$. This equation was used to fit the data in Figure 6 from 10 to 300 K. The data were not fitted below 10 K since it is generally not possible to model exchange coupling and zero-field splitting unambiguously when these effects are of similar magnitude, though we are continuing our efforts toward this goal following recent theoretical efforts that have been made to solve this problem.[31b] The refined isotropic g value, 2.128(2), is reasonable since the d^7 cobalt ions have a more than half-filled d orbital manifold. Since the four cobalt atoms pair up into sets of two which are ferromagnetically coupled at all temperatures, J is estimated to be >300 cm^{-1}. Because of the orbitally degenerate $^4T_1$ ground state of octahedral cobalt(II), spin−orbit coupling is expected to be large. The refined value of $2J'$ (0.85(1) cm^{-1}) appears to be artificially low because of these effects.

From the magnetic susceptibility data it is not possible to determine accurately the magnitudes of J or J', but we measured the molar magnetization of **2** at 2 K as a function of the applied field to confirm the $S = 6$ ground state. Unfortunately, the experimental magnetization curve (shown in Figure 7) is not saturated at 7 T, the high-field limit of our instrument. The value at 7 T reaches 9 μ_B mol^{-1}, which is consistent with a ground state with at least nine unpaired electrons.

Some tetranuclear complexes have shown interesting magnetic properties. For example, a very detailed magnetic study of the tetranuclear compound $Ni_4(OCH_3)_4(acac)_4(CH_3OH)_4$ has shown that this is a polynuclear ferromagnet with both intra- and intermolecular spin coupling.[5b] Also a particular class of manganese compounds with a Mn_4O_4 cubane-type core has been

---

(29) Kauffmann, K. E.; Popescu, C. V.; Dong, Y.; Lipscomb, J. D.; Que, L., Jr.; Münck, E. *J. Am. Chem. Soc.* **1998**, *120*, 8739.

(30) For a recent review on zero-field splitting in metal complexes, see: Boča, R. *Coord. Chem. Rev.* **2004**, *248*, 757.

(31) Palii, A. V.; Tsukerblat, B. S.; Coronado, E.; Clemente-Juan, J. M.; Borrás-Almenar, J. J. *Inorg. Chem.* **2003**, *42*, 2455. (b) Palii, A. V.; Tsukerblat, B. S.; Coronado, E.; Clemente-Juan, J. M.; Borrás-Almenar, J. J. *J. Chem. Phys.* **2003**, *118*, 5566.

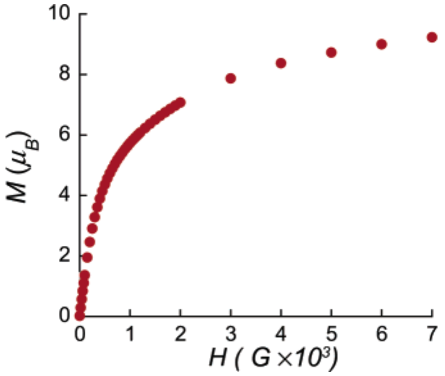

Figure 7. Plot of the magnetization of **2** versus field at a constant temperature of 2 K.

extensively studied because the molecules themselves exhibit properties like those of a magnet.[1b,32] This raises the question: Could compound **2** also be a single-molecule magnet? Certain qualities of **2** are akin to those of known single-molecule magnets: a high-spin ($S = 6$) ground state, molecular anisotropy (S_4 symmetry), and high magnetic anisotropy (large zero-field splitting). We measured the magnetic susceptibility of **2** using an alternating current to see if an out-of-phase signal (indicating slow magnetic relaxation or magnetic ordering) was present, but none was observed. Even though **2** does not exhibit single-molecule magnet behavior, this type of compound may be a useful building block for the synthesis of highly anisotropic species which may exhibit magnetic ordering.

Conclusions

The magnetic properties of the triangular compound **1** can be analyzed in the framework of a theoretical model that includes not only isotropic antiferromagnetic exchange interaction between Co ions and anisotropy of g-factors but also antisymmetric (AS) exchange acting within the ground manifold. This allowed us to fit the experimental data, although more precise determination of the AS exchange parameter requires analysis of the measurements on single crystals, which have not yet been possible. For **2**, the magnetic data show the presence of two pairwise ferromagnetic interactions. This allows modeling of the magnetic properties of the entire tetranuclear array by considering two dimers, each with $S = 3$, coupled through isotropic ferromagnetic exchange interaction. This model allows fitting in the temperature range 10−300 K, but the low-temperature data indicate the presence of significant orbital effects that are responsible for the drop of χT vs T. Although **2** does not display single-molecule magnetic behavior, it has features that may make it, or a related molecule, a precursor to a single-molecule magnet. It was mentioned in passing that a molecule analogous to **2** but with acac instead of DPM as the chelating ligand has long been known,[5b] but its magnetism was never investigated. Compound **2** is easier to make and easier to handle and has allowed a successful study of the magnetic properties of such a cuboidal Co_4O_4 structure.

Acknowledgment. We thank the NSF for support through a Nanoscale Science and Engineering/NIRT Grant (DMR 0103455) and the Telecommunications and Information Task Force of Texas A&M University, as well as the Welch Foundation. We also thank Dr. C. P. Berlinguette for helpful discussions. J.F.B. thanks the National Science Foundation for a predoctoral research fellowship.

Supporting Information Available: Crystallographic data for **1**, **2**, and Co(Hdepa)Cl_2 (CIF); tables of selected crystallographic data and bond distances and angles and a thermal ellipsoid plot of Co(Hdepa)Cl_2 (PDF). This material is available free of charge via the Internet at http://pubs.acs.org.

JA044185B

---

(32) Aliaga-Alcalde, N.; Edwards, R. S.; Hill, S. O.; Wernsdorfer, W.; Folting, K.; Christou, G. *J. Am. Chem. Soc.* **2004**, *126*, 12503.